



HAL
open science

Novel PET Nanocomposites of Interest in Food Packaging Applications and Comparative Barrier Performance With Biopolyester Nanocomposites

M.D. Sanchez-Garcia, E. Gimenez, J.M. Lagaron

► **To cite this version:**

M.D. Sanchez-Garcia, E. Gimenez, J.M. Lagaron. Novel PET Nanocomposites of Interest in Food Packaging Applications and Comparative Barrier Performance With Biopolyester Nanocomposites. *Journal of Plastic Film and Sheeting*, 2007, 23 (2), pp.133-148. 10.1177/8756087907083590 . hal-00572073

HAL Id: hal-00572073

<https://hal.science/hal-00572073>

Submitted on 1 Mar 2011

HAL is a multi-disciplinary open access archive for the deposit and dissemination of scientific research documents, whether they are published or not. The documents may come from teaching and research institutions in France or abroad, or from public or private research centers.

L'archive ouverte pluridisciplinaire **HAL**, est destinée au dépôt et à la diffusion de documents scientifiques de niveau recherche, publiés ou non, émanant des établissements d'enseignement et de recherche français ou étrangers, des laboratoires publics ou privés.

NOVEL PET NANOCOMPOSITES OF INTEREST IN FOOD PACKAGING APPLICATIONS AND COMPARATIVE BARRIER PERFORMANCE WITH BIOPOLYESTER NANOCOMPOSITES*

M.D. SANCHEZ-GARCIA,¹ E. GIMENEZ² AND J.M. LAGARON^{1,†}

¹*Novel Materials and Nanotechnology, IATA, CSIC, Burjassot, Spain*

²*Area of Materials, Department of Industrial Systems Engineering and Design, University Jaume I, Castellon, Spain*

ABSTRACT: Poly(ethylene terephthalate) (PET) is one of the polymers most widely used in the packaging industry. However, it is highly desirable to enhance its barrier properties for applications, such as carbonated drinks and other rigid and flexible packaging applications. The nanocomposites route offers unique possibilities to enhance the properties of this material, provided that adequate thermally resistant and legislation complying nano-additives are used. This study presents novel PET nanocomposites with enhanced barrier properties to oxygen, water, and limonene based on a new specifically developed food-contact-complying highly swollen montmorillonite grade, and, furthermore, presents and discusses morphological data. Moreover, given the current interest in the packaging industry to replace this material by other biopolyesters, a comparative barrier performance of PET nanocomposites versus that of biopolymers, such as poly(lactic acid) (PLA), polyhydroxyalkanoates (PHB, PHBV), and polycaprolactones (PCL) and their corresponding nanocomposites is also reported.

KEY WORDS: PET, food packaging, composites, barrier properties, biopolyesters.

*This is an expansion of a paper presented at the Society of Plastics Engineers' ANTEC 2007 conference held in Cincinnati, USA on May 6–10, 2007. Copyright SPE.

†Author to whom correspondence should be addressed. E-mail: lagaron@iata.csic.es
Figure 3 appears in color on line: <http://jpf.sagepub.com>

INTRODUCTION

POLY(ETHYLENE TEREPHTHALATE) (PET) is widely used due to its high transparency, high dimensional stability, and good thermal and mechanical properties. It is also frequently applied to produce fibers, films, and packaging materials which require intermediate barrier properties. Nevertheless, in many applications it is highly desirable to further enhance some properties, such as barrier properties for food packaging and beverages applications. A feasible way to do this is by using nanocomposites containing layered phyllosilicates [1].

Poly(ethylene terephthalate)-montmorillonite (MMT) nanocomposites with enhanced barrier properties have been reported previously in the literature. Some authors have reported $\approx 25\%$ oxygen permeability reductions for PET + 1%MMT by using *in situ* interlayer polymerization [2]. More recently, some authors have even claimed to obtain $\approx 94\%$ oxygen permeability reductions for PET + 5%MMT nanocomposites by using *in situ* polymerization [3]. Finally, $\approx 50\%$ water vapor permeability reduction for PET-MMT nanocomposites by melt blending in a rheometer was also reported [4].

Natural and organo-modified MMTs have thus been researched to a significant extent as reinforcing materials for polymers due to their high aspect ratio and unique intercalation/exfoliation characteristics by several processing routes. The most useful route to prepare PET-MMT nanocomposites is possibly the melt-compounding process because of its cost effectiveness and its enabling immediate implementation by converters using currently available processing machinery. However, due to the high temperatures needed for processing PET, the PET nanocomposites have become a major technological challenge due to potential degradation of the clay's organic modification during processing. In addition to this, legislation barriers are also imposing restrictions for MMT additives, because most commercially available organo-modified MMTs are not currently allowed for food contact.

Poly(ethylene terephthalate) is also facing a substantial threat arising from the increasing implementation of biodegradable and/or renewable biopolyesters, such as poly(lactic acid) (PLA), polycaprolactones (PCL), and polyhydroxyalkanoates (PHA). The reason for this is that these materials have excellent and promising properties that may replace conventional non-biodegradable polymers in a number of applications, including packaging, automotive, and biomedical applications [5].

The objective of this study was to characterize the morphology and barrier properties of a novel food-contact-complying PET

nanocomposite containing a 'highly swollen' organo-modified MMT grade. The study also reports comparative barrier data of PET and some biodegradable biopolyesters and of their corresponding nanocomposites.

MATERIALS AND METHODS

Materials

The PET resin used was a film extrusion grade supplied by the converter Neoplastica, Spain. No further details about the characteristics of the materials were provided.

The bacterial PHB grade was purchased from Goodfellow Cambridge Limited, UK, in powder form. The supplied PHB material with density 1.25 g/cm^3 is a melt-processable semi-crystalline thermoplastic polymer made by biological fermentation from renewable carbohydrate feedstocks. A melt-processable semi-crystalline thermoplastic polyhydroxybutyrate with 12 mol% valerate (PHBV) copolymer made by biological fermentation from renewable carbohydrate feedstocks was also purchased from the same manufacturer in pellet form.

The PCL grade FB100 was supplied in pellet form by Solvay Chemicals, Belgium. This grade has a density of 1.1 g/cm^3 and a mean molecular weight of 100,000 g/mol.

The semicrystalline PLA used was a film extrusion grade manufactured by Natureworks, USA (with a D-isomer content of $\approx 2\%$). The molecular weight had a number-average molecular weight (M_n) of $\approx 130,000 \text{ g/mol}$, and the weight-average molecular weight (M_w) was $\approx 150,000 \text{ g/mol}$.

A highly swollen food-contact-complying NanoterTM 2000 grade based on modified MMT was supplied by NanoBioMatters S.L., Spain. No further details on sample surface modification were disclosed by the manufacturer. The NanoterTM grade was characterized to be a very fine white powder with an average 3μ particle size. When the Nanoter 2000 grade was used with PHB and PHB/PCL resins, due to extensive hydrolytic degradation of the biopolymer, the compounds were extremely soft and thus of no use in packaging applications. Therefore, for the PHB and PHB/20% PCL nanocomposites a second food-contact-complying phyllosilicate grade called NanoterTM 2212 based on an organophilic surface modified kaolinite [6] supplied by NanoBioMatters S.L., Spain, was used.

Preparation of Nanocomposites

Prior to mixing, PET was dried at 60°C, under vacuum for 24 h to remove sorbed moisture in an oven under vacuum. PHBV, PLA, and PCL were dried at 70, 70, and 50°C, respectively. The polymers as well as the nanocomposite blends were prepared by melt-blending in an internal mixer (16 cm³ Brabender Plastograph) for 4 min at 260°C for PET and for 5 min at 175°C for PHBV, PLA, PHB, and PHB/20% PCL. The mixer was run at 60 rpm. The batch was manually removed from the mixing chamber and allowed to cool to room temperature in air. The resulting material was dried at the above-mentioned conditions. The samples were compressed into sheets (0.7 and 0.1 mm thick) in a hot-plate hydraulic press as follows:

- PET at 255°C and 2 MPa for 2 min.
- The biopolymers at 175°C and 2 MPa for 4 min.

The PET polymer sheets were crash cooled from the melt by rapid immersion in an ice bath. The biopolymer sheets were allowed to cool to room temperature under pressure. All the measurements and experiments were carried out on these polymer sheets.

The nanobiocomposite samples clay loading was 5 wt% unless otherwise stated.

Oxygen Transmission Rate

The oxygen permeability coefficient was derived from oxygen transmission rate (OTR) measurements recorded using an Oxtran 100 equipment (Modern Controls Inc., Minneapolis, MN, US). During all experiments temperature and relative humidity (RH) were held at 24°C and 0% RH and at 24°C and 80% RH. Relative humidity of 80% was generated by a built-in gas bubbler and was checked with a hygrometer placed at the exit of the detector. To avoid sample humidity equilibration during the actual OTR test at 80% RH and the subsequent fluctuations on barrier during the test, the samples were preconditioned at this RH by storage in a desiccator set at this RH by an appropriate salt solution. The samples were then purged with nitrogen for a minimum of 20 h prior to exposure to a 100% oxygen flow of 10 mL/min, and a 5 cm² sample area was measured by using an in-house developed mask. The permeability (*P*) coefficient was estimated from the steady-state OTR curve versus time. The samples were measured at least in duplicate and the data quoted corresponds as usual in permeability testing of non-industrial

samples to the lowest permeability value measured, as the scatter was rather small for the duplicates.

Gravimetric Measurements

Direct permeability to d-limonene of 95% purity (Panreac Química, Spain) was determined from the slope of the weight loss–time curves at 24°C and 40% RH. The films were sandwiched between the aluminum top (open O-ring) and bottom (deposit for the permeant) parts of a specifically designed permeability cell with screws. A Viton rubber O-ring was placed between the film and the bottom part of the cell to enhance sealability. Then the bottom part of the cell was filled with the permeant and the pinhole secured with a rubber O-ring and a screw. Finally, the cell was placed in the desired environment and the solvent weight loss through a film area of 0.001 m² was monitored and plotted as a function of time. Cells with aluminum films (with a thickness of ca. 10 μ) were used as control samples to estimate solvent loss through the sealing. The permeability sensibility of the permeation cells was determined to be better than $0.01 \times 10^{-13} \text{ kg} \cdot \text{m/s} \cdot \text{m}^2 \cdot \text{Pa}$ based on the weight loss measurements of the aluminum cells. Cells clamping polymer films but with no solvent were used as blank samples to monitor water uptake. Solvent permeation rates were estimated from the steady-state permeation slopes. Organic vapor weight loss was calculated as the total cell loss minus the loss through the sealing plus the water weight gain. The tests were done in triplicate and average values and standard errors are provided.

DSC Measurements

Differential scanning calorimetry (DSC) of PET and its nanocomposites was performed on a Perkin-Elmer (USA) DSC 7 thermal analysis system on typically 7 mg of material at a scanning speed of 10°C/min from room temperature to the melting point of the PET. Before evaluation, the thermal runs were subtracted from similar runs of an empty pan. The DSC equipment was calibrated using indium as a standard. Typically one sample of each material was tested.

SEM Measurements

For scanning electron microscopic (SEM) observation, the samples were fractured in liquid nitrogen and mounted on bevel sample holders. The fracture surface of the different samples was sputtered with Au/Pd

in vacuum. The scanning electron micrographs (Hitachi S4100, Tokyo, Japan) were taken with an accelerating voltage of 10 keV on the sample thickness.

TEM Measurements

Transmission electron microscopy (TEM) was performed using a JEOL 1010 (Jeol Ltd, Akishima, Japan) equipped with a digital Bioscan (Gatan) image acquisition system. TEM observations were performed on ultra-thin sections of microtomed nanocomposite sheets.

X-Ray Experiments

Wide angle X-ray experiments (WAXS) were performed using a Siemens D5000D (Germany) equipment. Radial scans of intensity versus scattering angle (2θ) were recorded at room temperature in the range $2\text{--}28^\circ$ (step size = 0.03° , scanning rate = 8s/step) with identical settings of the instrument by using filtered Cu $K\alpha$ radiation ($\lambda = 1.54 \text{ \AA}$), an operating voltage of 40 kV, and a filament current of 30 mA. To calculate the clay basal spacing, Bragg's law ($\lambda = 2d\sin\theta$) was applied.

RESULTS AND DISCUSSION

Morphology

Figure 1 shows scanning electron micrographs taken in criofractured cross-section specimens of the samples. The SEM examination reveals that a homogeneous distribution of the clays in the PET matrix and good interfacial adhesion must have been achieved for 5 wt% clay contents since no filler agglomerates and/or phase discontinuity can be discerned in the reinforced sample by this technique.

Figure 2 shows a typical TEM picture taken on specimens of the PET with 5 wt% Nanoter nanocomposite where the clay particles can be easily discerned. In nanocomposites, TEM and WAXS experiments are often used to discriminate the morphology of the nanofiller dispersion, since clay nanoparticles with high levels of dispersion, i.e., highly fractured tactoids, cannot be usually discerned by conventional SEM experiments. Figure 2 is representative of the morphology attained in the nanocomposite and indicates that this specimen does indeed exhibit a highly dispersed morphology consisting of exfoliated and some very thin intercalated layered clay nanoparticles. From the figure, the filler

Scanning electron micrographs (cross-section)

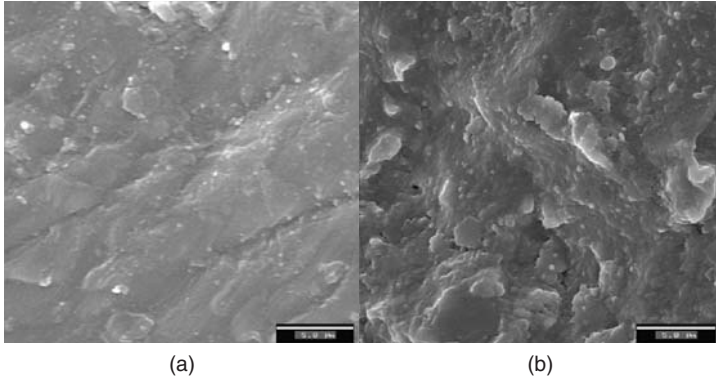


Figure 1. Scanning electron micrographs (cross-section): (a) melt blending of pure PET and (b) melt blending of PET with 5% Nanoter content.

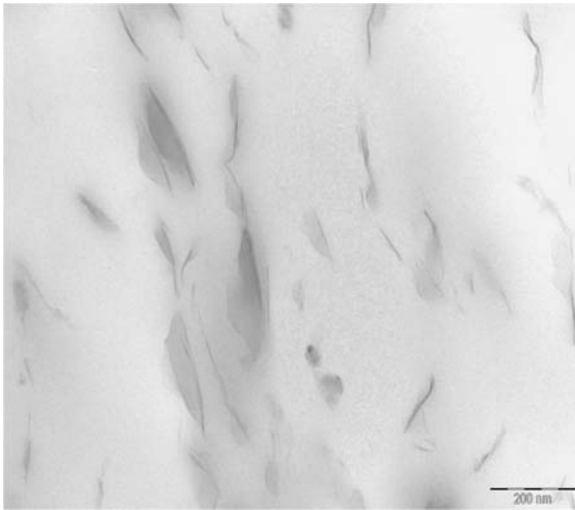


Figure 2. TEM photograph taken in a specimen of the PET + 5% Nanoter sample.

appears to be evenly dispersed across the matrix and remains in the nanometer range in the thickness direction. The corresponding WAXS patterns of the nanocomposite samples did not show evidence of the clay basal peaks, suggesting further that a very high dispersion in terms of intercalation and exfoliation of the filler has been achieved in the system (see Figure 3). Curiously, it is observed that the smallest (in length) clay

particles appear more exfoliated but fractured, whereas the intercalated thicker particles are more prone to remain in larger sizes in the length direction. It is well-known that a combination of appropriate surface modification and high shear forces in the melt during polymer processing, such as these generated in typical twin screw extruders, often lead to best results in terms of morphology in nanocomposites. In spite of the fact that the current study made use of moderate shear forces in the processing of the nanocomposites to potentially reduce processing-induced degradation in the systems, the morphology appears to still be quite favorable.

X-Ray Experiments

Figure 3 shows the WAXS patterns of the neat PET, PET+5% Nanoter, and of the Nanoter grade. The Nanoter MMT shows a basal spacing of $d_{001} = 39.4 \text{ \AA}$, indicating that the latter clay is very effectively swollen or expanded. The unmodified MMT was reported by the manufacturer to have a d basal spacing of $d_{001} = 11.9 \text{ \AA}$. Moreover, the modified clay shows two more peaks, besides the most intense one at

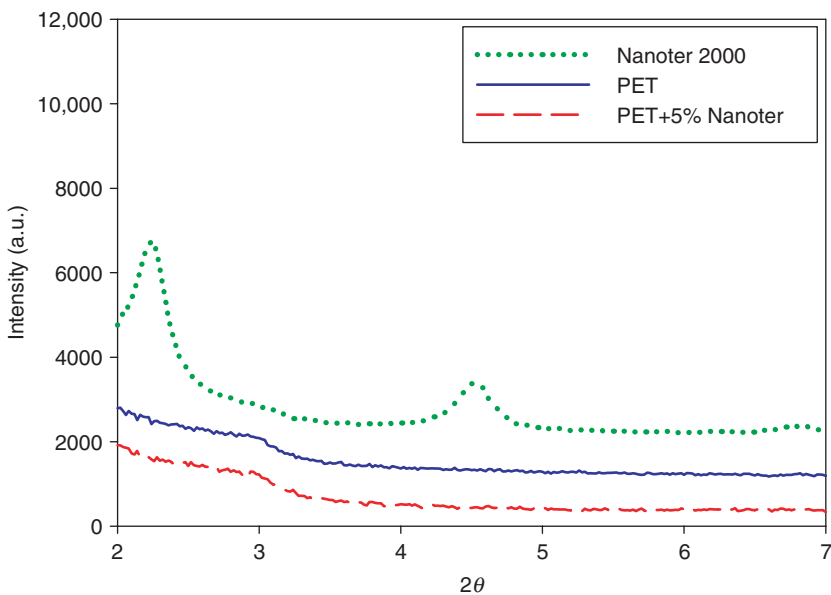


Figure 3. X-ray patterns of neat PET, PET + 5% Nanoter, and of the Nanoter powder.

2θ of 2.3° , at angles 4.6° and 6.9° . These diffraction peaks which decrease in intensity with increasing 2θ are associated to the second- and third-order diffraction features of the clay, respectively. From the high basal spacing results presented here, this highly swollen, ordered, and stacked layered modified structure is thought to lead to more easily dispersible clay morphologies in oil-based plastics. Figure 3 also indicates that the PET + 5% Nanoter sample shows no clay peaks in the range scanned as mentioned above, pointing that a high dispersion of the clay has been promoted across the polymer matrix as was anticipated by the TEM experiments.

Thermal Properties

Melting temperature (T_m), heat of fusion (ΔH_m), glass transition temperature (T_g), and heat capacity increment (ΔC_p), corrected for the clay content in the nanocomposite, were determined from the DSC first heating runs of the samples. The data are presented in Table 1 for all the samples. From the results, the enthalpy of fusion (calculated as the difference between the melting enthalpy and the cold crystallization enthalpy) appears to increase slightly in the PET + 5% Nanoter sample, albeit the differences may not be significant taking into account the error associated with the cold crystallization correction. The polymer T_g is higher in the nanocomposite and the jump in heat capacity is also slightly higher. The overall results suggest that crystallinity is not strongly affected in the PET + 5% Nanoter sample. Moreover, the thermal resistance, i.e., T_g , of the polymer is enhanced by $\approx 3^\circ\text{C}$ with the addition of Nanoter. In principle, crystallization of the nanocomposites is positive from a barrier perspective, since crystals are typically impermeable systems, but this may also impose additional rigidity and hence fragility to the nanocomposites mechanical performance.

Mass Transport Properties

Figure 4 shows, as an example, the OTR curves at 0% RH of the PET + 5% Nanoter sample and of the neat PET processed under

Table 1. DSC melting point, melting enthalpy, glass transition temperate, and heat capacity.

	T_m ($^\circ\text{C}$)	ΔH_m (J/g)	T_g ($^\circ\text{C}$)	ΔC_p (J/g $^\circ\text{C}$)
PET	245	18	69	0.3
PET-5% Nanoter	245	22	72	0.4

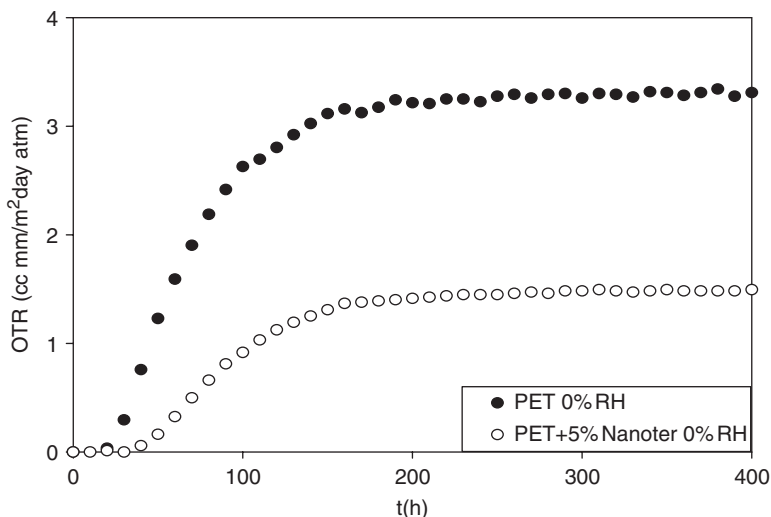


Figure 4. Oxygen transmission rate curve of the pure PET and of the PET + 5% Nanoter at 0% RH.

the same conditions. From this figure, it is seen that the equilibrium transmission rate is higher in the unfilled blend than in the nanocomposite indicating that a lower permeability is clearly reached in the nanocomposite systems, and that the diffusion is clearly faster in the unfilled blend. Table 2 shows the calculated oxygen permeability coefficients, water permeability, and limonene permeability for the samples of PET. From this table, it is seen that the oxygen permeability of the nanocomposite of PET is reduced by $\approx 55\%$ at 0% RH in the 5% Nanoter compared to the pure PET sample. The table also shows that at higher RH (80%), the oxygen barrier is somewhat lower in the neat polymer compared to dry conditions and the permeability reduction is $\approx 35\%$. A previous study [8] reported that the oxygen permeability for PET is of $\approx 4.11 \times 10^{-19} \text{ m}^3 \cdot \text{m/s} \cdot \text{m}^2 \cdot \text{Pa}$ when measured at 0% RH, a value which is similar to the permeability measurement taken in the laboratory.

Water and limonene direct permeability were also evaluated for the PET and for their nanocomposites and are summarized in Table 2. This table also shows water and limonene permeability measured in samples containing 1 wt% of clay. Films of PET with 1% wt Nanoter have a limonene permeability decrease of 26% compared to the unfilled material, but the sample with 5% wt Nanoter content has a reduction in limonene permeability of ca. 68%. A reduction in water permeability of $\approx 43\%$ is observed in the nanocomposite of PET with 1% wt Nanoter

Table 2. Oxygen permeability at 0 and 80%RH and d-Limonene and water permeability.

	PO_2 ($m^3 \cdot m/m^2 \cdot s \cdot Pa$) 24°C, 80% RH	PO_2 ($m^3 \cdot m/m^2 \cdot s \cdot Pa$) 24°C, 0% RH	P limonene ($kg \cdot m/s \cdot m^2 \cdot Pa$)	P water ($kg \cdot m/s \cdot m^2 \cdot Pa$)
PET	$4.26 e^{-19}$	$3.78 e^{-19}$	$1.17 \pm 0.15 e^{-13}$	$0.03 \pm 0.01 e^{-13}$
PET + 1% Nanoter	—	—	$0.87 \pm 0.55 e^{-13}$	$0.017 \pm 0.002 e^{-13}$
PET + 5% Nanoter	$2.81 e^{-19}$	$1.69 e^{-19}$	$0.37 \pm 0.07 e^{-13}$	$0.026 \pm 0.0009 e^{-13}$
Literature value PET	$4.45 e^{-19}$ [8] 85% RH	$4.11 e^{-19}$ [5]	$0.000048 e^{-13}$ [7] 23°C-40 Pa	$0.028 \pm 0.00015 e^{-13}$ [13] 37.8°C-100% RH
PLA	$22.1 e^{-19}$	$22.6 e^{-19}$	—	$0.126 \pm 0.010 e^{-13}$
PLA + 5% Nanoter	$15.4 e^{-19}$	$19.5 e^{-19}$	—	$0.104 \pm 0.009 e^{-13}$
Literature value PLA	$17.5 e^{-19}$ [10]	—	—	$0.130 e^{-13}$ [5]
PHBV	—	$15.7 e^{-19}$	$1.99 \pm 1.01 e^{-13}$	$0.069 \pm 0.003 e^{-13}$
PHBV + 5% Nanoter	—	$11.5 e^{-19}$	$1.27 \pm 0.08 e^{-13}$	$0.032 \pm 0.002 e^{-13}$
Literature value PHBV	—	—	—	$0.070 e^{-13}$ [5]
PHB	—	$2.24 e^{-19}$	$0.088 e^{-13}$	$0.017 \pm 0.0009 e^{-13}$
PHB + 5% Nanoter	—	$1.78 e^{-19}$	$0.01 \pm 0.0005 e^{-13}$	$0.016 \pm 0.00003 e^{-13}$
PHB/20% PCL	$5.19 e^{-19}$	$4.2 e^{-19}$	—	$0.025 \pm 0.0003 e^{-13}$
PHB/20% PCL + 5% Nanoter	$2.80 e^{-19}$	$2.4 e^{-19}$	—	$0.021 \pm 0.0005 e^{-13}$

but films of PET with 5% wt Nanoter have a reduction in water permeability of only 14%. The reason for the latter counterintuitive behavior in the water permeability behavior could be related to the inherent MMT clay hygroscopicity. Previous studies reported that the PET limonene permeability is about $0.0000048 \times 10^{-13} \text{ kg} \cdot \text{m/s} \cdot \text{m}^2 \cdot \text{Pa}$ when measured at 23°C and 40 Pa [7]. The reason for the large disagreement with the limonene permeability data could be related to the different origins of the two samples (extruded vs. un-oriented compression molded specimens) and the fact that the polymer grade, the test conditions used, and the differences in partial pressure used for testing were largely different. Since the differences in partial pressure gradient used for testing was much smaller than the ones reported here, the sample is expected to be much less plasticized by the component ingress. On the other hand, the PET water permeability was earlier reported to be about $0.028 \times 10^{-13} \text{ kg} \cdot \text{m/s} \cdot \text{m}^2 \cdot \text{Pa}$ when measured at 37.8°C and 100% RH [9], a value which is similar to the one measured in the laboratory. This is likely to be so because the test conditions were more alike for the evaluation of the transport properties of this permeant.

Figure 5 shows the comparative oxygen permeability data for PET and several thermoplastics biopolymers and their nanocomposites at 0%RH. Further details about the biopolymers morphology, thermal and mechanical and other relevant properties will be published elsewhere, e.g., [6]. Table 2 also compares the barrier performance of these biopolyesters and their corresponding nanobiocomposites. All the biopolymer specimens were obtained by slow cooling from the melt (unlike PET that was rapidly quenched) and thus had enhanced crystallinity [6]. From the permeability results, only PHB and PHB nanocomposites show lower oxygen permeability than the pure PET. The PHB nanocomposite has the lowest oxygen permeability value of all biodegradable materials, and becomes closer to the PET nanocomposite. The PHB/20% PCL nanocomposite also shows lower oxygen permeability than the pure PET. The biodegradable materials (PHBV and PLA) have higher oxygen permeability compared to PET, and their nanobiocomposites have better oxygen barrier than the neat biopolymers.

Figure 6 compares water and limonene permeability for PET and biodegradable polymers and their nanocomposites. Table 2 also compares the vapor barrier performance of the biopolyesters and their corresponding nanobiocomposites. PHB and the PHB nanocomposite show better water and aroma (limonene) barrier compared with PET. The PHB nanocomposite has the lowest water permeability and the limonene permeability values of it are much lower than that of

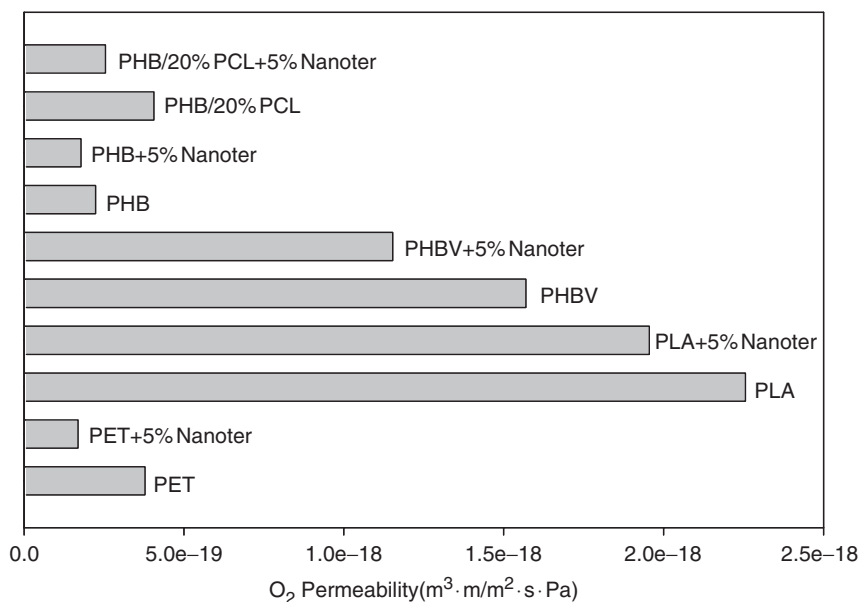


Figure 5. Pure PET, PET + 5% Nanoter, and biopolyesters with their nanocomposites containing 5 wt% Nanoter oxygen permeability at 0% RH.

the PET nanocomposite. The PHBV nanocomposite has water permeability similar to the neat PET and the limonene permeability of this nanocomposite is also close to that of the neat PET.

In summary, the PHB and PHB/20% PCL nanobiocomposites show the best barrier properties of all biopolyesters. These materials additionally show lower water and limonene permeability than both pure PET and the PET nanocomposite. For oxygen permeability the PET nanocomposites show the best barrier performance of all the materials considered.

CONCLUSIONS

This study demonstrates that the oxygen, limonene, and water barrier of PET can be improved by blending with 5 wt% or less of the novel food-contact-complying highly swollen MMT system used. The permeability was seen to generally decrease with increasing MMT content, as would be expected. This effect is thought to be chiefly ascribed to the clay platelets, which are thought to promote increased tortuosity (τ) or detour factors in the diffusion of the materials and,

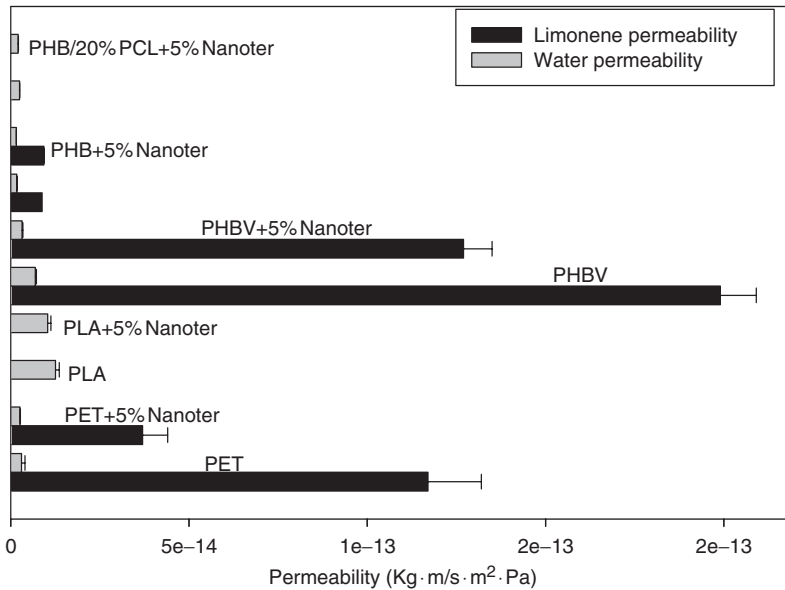


Figure 6. Limonene and water permeability of pure PET and PET + 5% Nanoter and of the biopolyesters and their nanocomposites containing 5 wt% Nanoter.

therefore, lead to lower permeability. This work also suggests that the PHB and the PHB/PCL blend nanobiocomposites show better water, aroma (limonene), and oxygen barrier than pure PET. Nevertheless, the PET nanocomposites' oxygen permeability is the lowest of all materials considered.

The nanoclay dispersion is known to have a strong role in the barrier properties. Thus, exfoliated systems with platelet orientation in the flow direction are expected to yield optimum barrier performance. Crystallinity also plays an important role in promoting barrier properties; however, since crystallinity was not seen to increase significantly in the PET system studied here, the observed permeability reduction is therefore directly ascribed to the highly dispersed clay morphology in the polymer.

ACKNOWLEDGMENTS

The authors would like to acknowledge NanoBioMatters S.L., Paterna Spain for supplying clays. The EU integrated project SUSTAINPACK and the Spanish MEC project MAT2006-10261-C03-01 are also

acknowledged for financial support. Finally, M.D.S.G. would like to thank the FPI program of the GV associated to the CYCIT projects MAT2003-08480-C3 for the research grant.

REFERENCES

1. Hao, J., Lu, X., Liu, S., Lau, S.K. and Chua, Y.C. (2006). Synthesis of Poly(ethylene terephthalate)/Clay Nanocomposites using Aminododecanoic Acid-modified Clay and a Bifunctional Compatibilizer, *J. Appl. Polym. Sci.*, **101**(2): 1057–1064.
2. Ke, Z. and Yongping, B. (2005). Improve the Barrier Property of PET Film with Montmorillonite by *in situ* Interlayer Polymerization, *Materials Letters*, **59**(27): 3348–3351.
3. Choi, W.J., Kim, H.-J., Yoon, K.H., Kwon, O.H. and Hwang, C.I. (2006). Preparation and Barrier Property of Poly(ethylene terephthalate)/Clay Nanocomposite using Clay-supported Catalyst, *J. Appl. Polym. Sci.*, **100**(6): 4875–4879.
4. Vidotti, S.E., Chinellato, A.C., Boesel, L.F. and Pessan, L.A. (2004). Poly (ethylene terephthalate)-organoclay Nanocomposites: Morphological, Thermal and Barrier Properties, *J. Metastable and Nanocrystalline Materials*, **22**(1): 57–64.
5. Cava, D., Giménez, E., Gavara, R. and Lagaron, J.M. (2006). Comparative Performance and Barrier Properties of Biodegradable Thermoplastics and Nanobiocomposites versus PET for Food Packaging Applications, *J. Plas. Film and Shtg*, **22**(4): 265–274.
6. Sanchez-Garcia, M.D., Gimenez, E. and Lagaron, J.M. Morphology and Barrier Properties of Novel Nanobiocomposites of Bacterial Poly(3-hydroxybutyrate), Poly(ϵ -caprolactone) and Layered Silicates, *Carbohydrate Polymers*, In Press, DOI: 10.1016/j.carbpol.2007.05.041.
7. Auras, R., Harte, B. and Selke, S. (2005). Sorption of Ethyl Acetate and d-limonene in Poly(lactide) Polymers, *J. Sci. Food Agric.*, **86**(4): 648–656.
8. Hua, Y.S., Prattipatia, V., Mehtab, S., Schiraldia, D.A., Hiltner, A. and Baer, E. (2005). Improving Gas Barrier of PET by Blending with Aromatic Polyamides, *Polymer*, **46**(8): 2685–2698.
9. Rafael, A., Auras, S., Singh, P. and Singh, J.J. (2005). Evaluation of Oriented Poly(lactide) Polymers vs. Existing PET and Oriented PS for Fresh Food Service Containers, *Packgg. Technol. Sci.*, **18**(4): 207–216.
10. Petersen, K., Nielsen, P.V. and Olsen, M.B. (2001). Physical and Mechanical Properties of Biobased Materials, *Starch*, **53**(8): 356.

11. Hiltner, A., Liu, R.Y.F., Hu, Y.S. and Baer, E. (2005). Oxygen Transport as a Solid-state Structure Probe for Polymeric Materials: A Review, *J. Polym. Sci.: Part B: Poly. Phys.*, **43**(9): 1047–1063.

BIOGRAPHIES

M. Dolores Sanchez-Garcia

M.D. Sanchez-Garcia is a PhD student at the Institute of Agrochemistry and Food Technology (IATA), Spanish Council for Scientific Research (CSIC). She graduated in Chemistry from the University of Valencia, Spain.

Enrique Gimenez

E. Gimenez is a Professor of Materials Science at the University Jaume I, Castellon. He graduated in Industrial Engineering from the Polytechnic University of Valencia and received a PhD from the University of Castellon, Spain. He is a scientific advisor at NanoBioMatters Ltd., Paterna, Spain.

Jose M. Lagaron

J.M. Lagaron is senior research scientist and founder of the group Novel Materials and Nanotechnology at IATA, CSIC. He graduated in Chemistry and obtained his PhD in Polymer Physics from the University of Valladolid, Valladolid, Spain. He worked for five years as research associate in research centers of the petrochemical companies DSM Research, The Netherlands and BP Chemicals, UK and he is currently scientific advisor at NanoBioMatters Ltd, Paterna, Spain.